Moons, J.; de Azambuja, F.; Mihailović, J.; Kozma, K.; Smiljanić, K.; Amiri, M.; Ćirković-Veličković, T.; Nyman, M.; Parac-Vogt, T. Discrete Hf18 Metal-oxo Cluster as a Heterogeneous Nanozyme for Site-Specific Proteolysis. *Angewandte Chemie (International Edition)* **2020**, *59* (17), 1–9. https://doi.org/10.1002/anie.202001036.

Discrete Hf_{18} metal-oxo cluster as a heterogeneous nanozyme for site-specific proteolysis

Jens Moons[a], Francisco de Azambuja[a], Jelena Mihailovic[b], Karoly Kozma[c], Katarina Smiljanic[b], Mehran Amiri[c], Tanja Cirkovic-Velickovic[b,d,e,f], May Nyman[c], Tatjana N. Parac-Vogt*[a]

Abstract: Effective heterogeneous catalysts for the controlled transformation of large and complex biomolecules are rare and challenging to develop. In particular, selective hydrolysis of proteins by non-enzymatic catalysis is difficult to achieve, yet it is crucial for many modern applications in biotechnology and proteomics. Herein we report that discrete hafnium metal-oxo cluster $[Hf_{18}O_{10}(OH)_{26}(SO_4)_{13}(H_2O)_{33}]$ (**Hf_{18}**), which is centred by the same hexamer motif found in many MOFs, acts as a heterogeneous catalyst for the efficient hydrolysis of horse heart myoglobin (HHM) protein in low buffer concentrations. Remarkably, among 154 amino acids present in the sequence of HHM, strictly selective cleavage at only 6 solvent accessible aspartate residues, Asp5, Asp21, Asp45, Asp110, Asp123 and Asp142 was observed. Mechanistic experiments suggest that the hydrolytic activity is likely derived from the synergistic actuation of Hf^{4+} Lewis acidic sites and the Brønsted acidic surface of **Hf_{18}**. A combination of X-ray scattering and ESI-MS revealed that **Hf_{18}** is completely insoluble in these conditions, confirming the HHM hydrolysis is caused by a heterogeneous reaction of solid **Hf_{18}** cluster, and not from smaller, soluble Hf species that could leach in solution. This study highlights the great potential of discrete metal-oxo cluster materials as inorganic proteases.

Introduction

Protein hydrolysis is a crucial step in the analysis of the proteome, which is defined as the complete set of proteins produced by living cells, tissues or organisms under a specific time and defined conditions. The proteome represents the end result of gene transcription, translation, and protein synthesis up to post-translational protein modifications (PTM), and thereby its understanding is of essential importance in various areas of biological and biomedical research. Currently protein hydrolysis is mainly achieved by using trypsin, which is active under a narrow window of temperature and pH conditions (37 °C, buffered systems with specific ionic prerequisites). Such strict requirements prompted extensive research towards developing more robust proteases, leading to chemically altered trypsins more resistant to autolysis and denaturing conditions,[1,2] or immobilization on different solid substrates, such as magnetic nanoparticles[3], polyacrylamide matrices[4] and glyoxal-agarose[5]. Although immobilization of trypsin has been proven to be a viable strategy to industrial purposes, the consistent use of trypsin has narrowed the 'vision' in bottom-up proteomics analyses. Nearly 96 % of the deposited peptides in databases originate from trypsin, and have a short length averaging 6 amino acids, consequently providing restricted insight of the analysed proteomes.[6]

In this context, we have been interested in exploring Lewis acidic metal-oxo clusters as a middle-term solution for traditional biochemistry tools, namely the aforementioned sensitive enzymatic reactions or the long known harsh chemical agents,[7–9] to overcome the loss of very specific information such as isoform determination or PTM location and identification. More specifically, we have pioneered metal-substituted polyoxometalates (POMs) as a new class of artificial proteases. POMs comprise a large class of metal-oxygen clusters that are rich in structural and configurational diversity and nuclearity, electronic and/or magnetic properties, acid or basic nature and widely ranging charge density.[10–12] The incorporation of strong Lewis acid metals such as Ce(IV), Zr(IV) and Hf(IV) in POMs stabilizes them in aqueous solutions at neutral pH, and enables leveraging their Lewis acidity to the hydrolysis of several proteins[13–17] and shorter peptides[18–20]. Furthermore, the fragments generated by POM catalysts are in the range from 5-15 kDa, which is ideal for middle-down proteomics applications, therefore their analysis could increase sequence coverage in addition to information provided by trypsin digestion.

Even though metal-substituted POMs show potential as fully homogenous artificial proteases, their use in proteomics is hindered due to difficulty in separating them from the protein digest.[21] To overcome this challenge, we turned our attention to the design of inexpensive and easily removable heterogeneous catalysts that mimic enzymatic processes. Such materials experienced an explosive growth in the past decade, and many metal-containing nano-materials with enzyme-like characteristics ("nanozymes") have been described in recent years.[22] They have been mainly reported to catalyse redox reactions such as the oxidative cleavage of human serum albumin (HSA),[23] or to exhibit peroxidase, oxidase, superoxidase and catalase-like activities.[24] However, nanozymes have been far less explored as catalysts for hydrolysis reactions, and mainly the phosphoester bond cleavage in nucleic acids (or their model systems)[25,26], and in chemical warfare agents has been reported.[22] On the other hand, very few examples of 'nanozyme'-catalysed peptide bond hydrolysis in proteins have been reported.[27]

Group IVA materials are used in biomedical, biosensing and microelectronics applications.[28–30] Moreover, the Hf-tetramer

[a] J. Moons, Dr. F. de Azambuja, Prof. T. N. Parac-Vogt*
Department of Chemistry, KULeuven
Celestijnenlaan 200F, 3001 Leuven, Belgium
E-mail: tatjana.vogt@kuleuven.be

[b] J. Mihailovic, dr. K. Smiljanic, Prof. T. Cirkovic-Velickovic
Faculty of Chemistry, University of Belgrade
Studentski trg 16, 11 000 Belgrade, Serbia

[c] K. Kozma, M. Amiri, Prof. M. Nyman
Department of Chemistry, Oregon State University
Corvallis, OR 97331-4003, United States

Prof. T. Cirkovic-Velickovic
[d] Ghent University Global Campus, Incheon, South Korea
[e] Ghent University, Faculty of Bioscience Engineering, Ghent, Belgium
[f] Serbian Academy of Sciences and Arts, Belgrade, Serbia

Supporting information for this article is given via a link at the end of the document.

$[Hf_4(OH)_8(H_2O)_{16}]^{8+}$ that is ubiquitous in Hf aqueous acid solutions is used in high resolution nanolithography.[31–33] Self-assembly and properties of Group IV clusters can be tuned with strong ligands such as sulphate and peroxide.[33–35] The **Hf_{18}** polynuclear cluster $[Hf_{18}O_{10}(OH)_{26}(SO_4)_{13}(H_2O)_{33}]$ (Figure 1) in particular is an important intermediate between Hf sulphate−peroxide thin film deposition solutions and dielectric HfO_2 thin films and hard masks.[36] The **Hf_{18}** cluster readily precipitates from solutions containing H_2O_2, H_2SO_4, and '$HfOCl_2$' (the commercial form of Hf_4). First structurally reported in 1975,[37] **Hf_{18}** is centred by the same Hf_6-hexamer motif (Hf_6) that is the building block of stable MOFs, including prior-studied MOF-808 and UiO-66.[38] Hf_6 shares opposite edges with two Hf pentamers, and six additional edge-sharing Hf polyhedra bridge the pentamers of the elongate pentamer−hexamer−pentamer unit. The periphery of the **Hf_{18}** structure is capped by thirteen sulphate anions, resulting in the neutral nanostructure which is completely insoluble in water. In addition, ten of the eighteen Hf-centres have labile terminal water molecules that can deprotonate or be replaced with a different ligand such as a carboxylic acid. Thus the **Hf_{18}** is both a Lewis and a Brønsted acid, which are desired properties for the activation of the peptide bond.[39] Furthermore, **Hf_{18}** is a discrete species with well-defined formula and structure, and therefore provides the opportunity to correlate structure and properties to interaction and reactivity towards protein substrates. Considering the challenges associated with protein hydrolysis, especially by heterogeneous materials, and the unique features of **Hf_{18}** derived from its chemical composition and structure, we set out to investigate its protease activity. In this work, we evaluate the reactivity of the **Hf_{18}** cluster towards Horse Heart Myoglobin (HHM, a globular protein consisting of 154 amino acids) and examine molecular interactions between the protein and the **Hf_{18}** nanocluster.

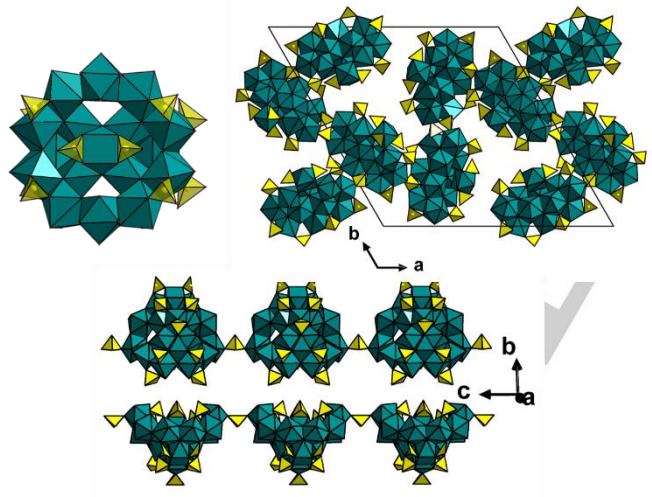

Figure 1. Views of **Hf_{18}**, Upper left: the isolated $[Hf_{18}O_{10}(OH)_{26}(SO_4)_{13}\cdot(H_2O)_{33}]$ cluster. Upper right: unit cell view down the c-axis. Void spaces contain solvent molecules. Bottom: emphasizing connectivity of **Hf_{18}**-chains along the *c*-axis, explaining its insolubility. Hafnium polyhedra are teal, sulfate polyhedra are yellow.

Results and Discussion

Hydrolysis of Horse Heart Myoglobin (HHM) by Hf_{18}

The protease activity of **Hf_{18}** cluster was probed using HHM as a model protein substrate. HHM is a globular, iron-heme-containing protein (154 amino acids, 16.951 kDa) that facilitates oxygen supply and movement within muscles and scavenges intracellular NO. With an isoelectric point of 6.80-7.20, HHM carries a slight positive charge under physiological pH conditions.[40–42] To investigate the hydrolysis of HHM, 2 µmol of solid **Hf_{18}** was suspended in 1 mL 0.02 mM HHM solution, resulting in a 1:100 molar ratio of protein:**Hf_{18}**, at 37 and 60°C. As low activity was observed at 37 °C, the remaining experiments were carried out at 60 °C (See Figure S1). The **Hf_{18}** is a microcrystalline solid that is insoluble in all media,[36] thus the catalytic reactions are heterogeneous. Three different solutions were investigated: samples A and B were suspended in 20 mM of HEPES and phosphate buffer, respectively, and sample C was suspended in water (Scheme 1). HEPES and phosphate buffer were selected as representative buffers commonly used in protein research. Whereas HEPES exhibits low affinity towards Lewis acidic metals, the coordinating affinity of phosphate buffer is much larger and will be addressed later in this study. As references, three blank reactions under the respective conditions but lacking **Hf_{18}** cluster were also prepared and run in parallel to samples A-C. For all conditions, the pH was adjusted to 7.4 prior to reaction.

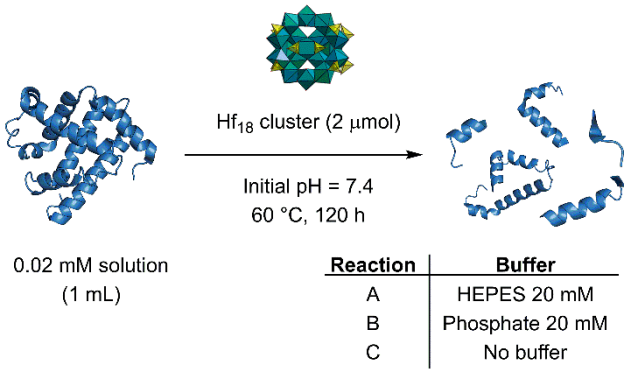

Scheme 1. Protease activity of Hf18 cluster was studied using Horse Heart Myoglobin (HHM) as a model protein substrate in two buffered and one unbuffered conditions. Incubation conditions: 1.0 mL 0.02 mM HHM solution, 2 µmol of solid Hf18, pH = 7.4, 60 °C, 120 h. In two conditions, protein was suspended in buffer (Hepes or phosphate, concentration 20 mM).

The progress of the hydrolysis reaction was followed by sodium dodecyl sulphate polyacrylamide gel electrophoresis (SDS-PAGE). After mixing of Hf_{18} and HHM, the intensity of the brown red colour originating from HHM faded, indicating disappearance of HHM from solution, most likely due to the adsorption of HHM to Hf_{18} surface (see "Interaction" discussion below). Due to these strong interactions, to render samples suitable for SDS-PAGE analysis we needed to develop a method to re-dissolve the HHM and its fragments. After specific time increments, the supernatant solution was separated from the HHM-Hf_{18}

precipitate by centrifugation. The precipitate was incubated in 200 µL of a 1 % aqueous ammonia solution for 2-4 hours at room temperature, which resulted in ca. 90-95 % recovery of HHM and its fragments. The reaction was monitored for 120 hours, but in 2 hours of reaction the presence of multiple fragments was observed, and their intensity increased over time. The emergence of distinct peptide bands with similar lower molecular weight observed in all three catalysed samples suggested that selective hydrolysis of HHM took place with an analogous cleavage pattern. In contrast, no hydrolysis was observed in the absence of Hf_{18} cluster even after 120 h of incubation. (Figure 2)

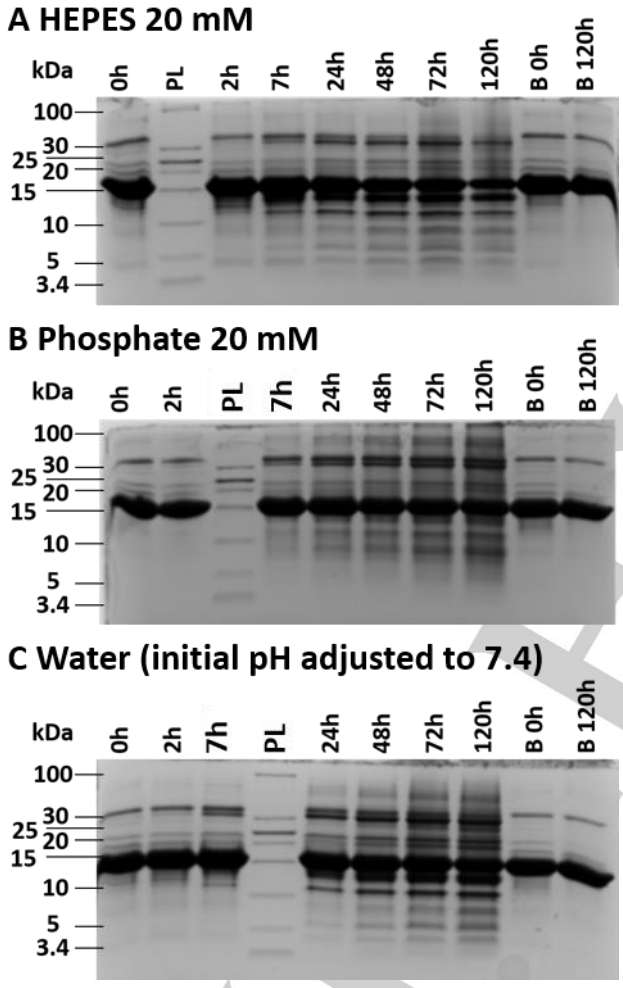

Figure 2. Coomassie blue stained SDS-PAGE of 0.02 mM horse heart myoglobin hydrolyzed by 2 µmol **Hf_{18}** at 60°C in 3 different buffers. A: HEPES buffer: 20 mM, pH 7.4; B: phosphate buffer: 20 mM, pH 7.4; C: water: pH adjusted to 7.4 with NaOH. All Blank (identified by a B on the right side of SDS-PAGEs) samples were made under the respective conditions only lacking **Hf_{18}**. PL: protein ladder

Due to the expected Brønsted acidity of **Hf_{18}**, the pH of all reaction mixtures was measured after 2 hours of incubation at 60 °C, and a significant decrease of the pH from 7.4 to ca. 3.0 was observed in all 3 samples. The same decrease in pH of solution was observed in the absence of HHM indicating that the protons released in solution originate from the **Hf_{18}** cluster. This large decrease can be attributed to partial dissociation of labile terminal water molecules present on 10 out of the 18 Hf centres.[43] If all terminal water ligands would dissociate a pH value of ≈1.50 could be reached for 2 µmol Hf_{18} (see SI for details). However, the pH stabilizes at 3.0 during the reaction, indicating that only partial dissociation occurs.

Increasing the buffer capacity of HEPES buffer to 50 mM resulted in a reaction mixture consisting of **Hf_{18}** and HHM having pH of 4.3 after 2 hours (See Table S1). This reaction mixture was also analysed by SDS-PAGE and while the pattern of observed fragments did not change, the yield of HHM hydrolysis was clearly lower than when 20 mM buffer was used (See Figure S2A). Further increasing the buffer concentration to 100 or 200 mM, resulted in stable pH of solutions that were close to neutral (See Table S1); however, the complete inhibition of HHM hydrolysis was observed in these reaction mixtures (See Figure S2B-C). These results suggest that the acidity of the **Hf_{18}** surface, which could be neutralized in strongly buffered solutions, is necessary for HHM hydrolysis to occur.

To identify the cleavage sites of the fragmentation pattern observed in SDS-PAGE experiments, the reactions were further analysed by HPLC-MS/MS analysis. Overall, highly selective cleavage of HHM by **Hf_{18}** at six aspartate residues (abbreviated as D) (D5, 21, 45, 110, 123, 142 – indicated with red arrows in Figure 3A) was detected by LC-MS/MS spectra analysis of full samples (Figure 3A). These cleavages sites were further confirmed by complimentary approaches using pre-fractionation of the samples or in-gel digestion. In addition, such complimentary approaches did not reveal additional cleavage sites (a complete set of results and full sample preparation is available in the SI). Interestingly, both the Asp-X and X-Asp cleavage patterns were observed, in contrast to previously reported hydrolysis of HHM by Zr(IV)-POMs, which was Asp-X specific (Figure 3B).[15] Moreover, **Hf_{18}** cleaved positions D110 and D123 located in negatively charged regions of proteins, which is strikingly distinct from the positive surface charge driven hydrolysis observed previously. Such distinct features observed with **Hf_{18}** likely derive from its Brønsted acidity, which affects the protein conformation and could make such residues more accessible than in previous reactions (see discussion below). This new selectivity also shows how a fine tuning of the metal-oxo cluster chemical properties can be useful to design artificial proteases targeting different regions of the proteins.

The mechanism of HHM hydrolysis by Hf_{18} cluster.

The high HHM hydrolysis efficiency and Asp-selectivity of Hf_{18} in derives from its heterogeneous form combined with its Lewis and Brønsted acidity, as evidenced by our comprehensive mechanistic study. Hf_{18} preferential cleavage of X-Asp and Asp-X peptide linkages likely proceeds through the formation of a key labile hemiaminal intermediate, following a similar mechanism to

the previously reported Asp selective hydrolysis of proteins and model peptides mediated by Brønsted acids.[44,45] In this reaction

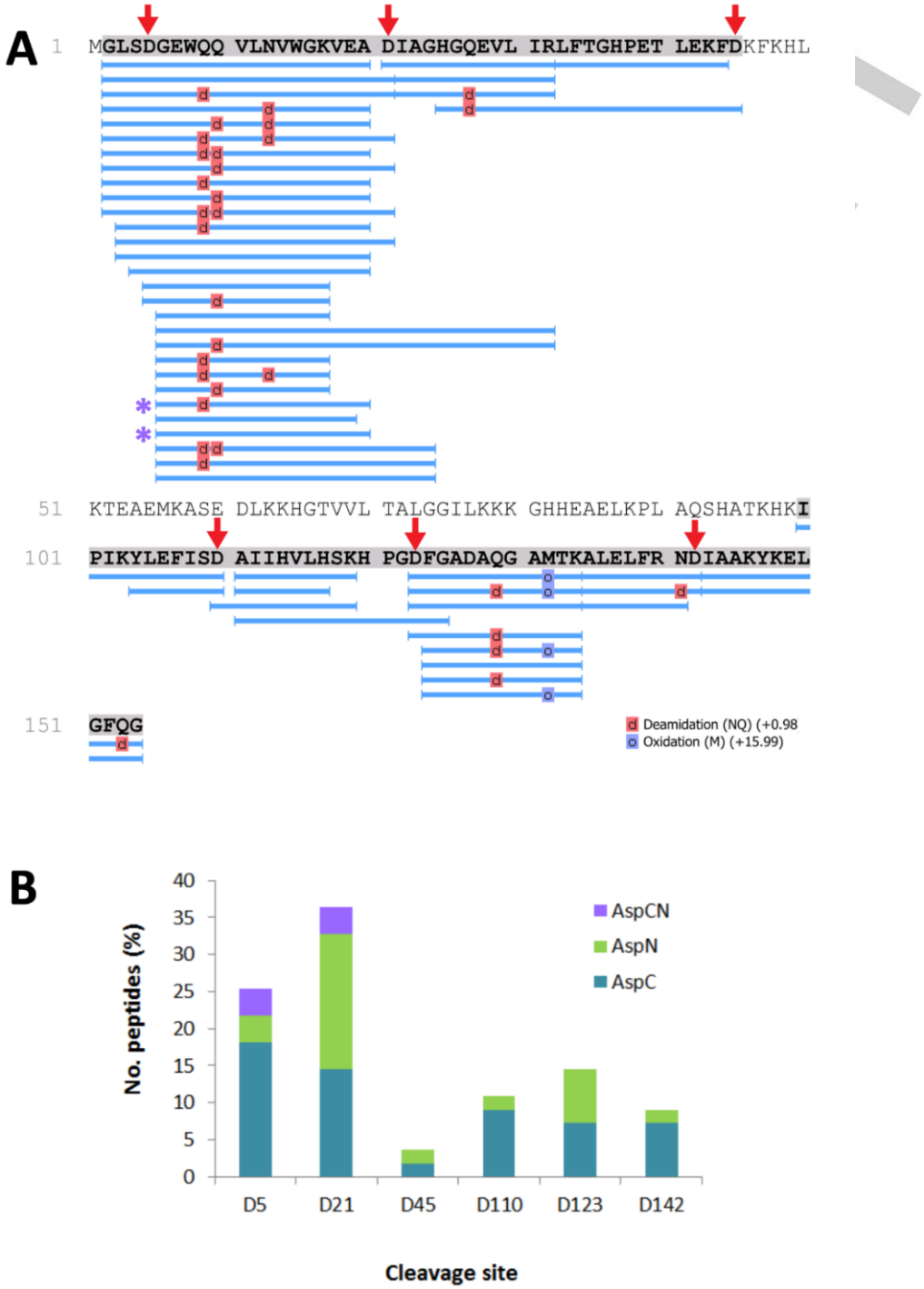

Figure 3 Hf_{18} cleavage of myoglobin (accession number P68082, MYG_HORSE) by Hf_{18}: **A.** Coverage of myoglobin sequence by Hf_{18} generated peptides; red arrows indicate Hf_{18} generated cleavage sites, purple asterisks indicate peptides that are cleaved at both Asp termini; grey shaded letters represent parts of covered AA sequence; blue bars indicate myoglobin peptides that are the result of Hf_{18} hydrolysis; **B.** Cleavage site frequency showing number of peptides (%) detected per cleavage site, categorized as cleavage at Asp N-terminus (AspN), C-terminus (AspC) or both (AspCN). Two discovered AspCN peptides span the sequence between D5 and D21, and are shown as shared between the two sites

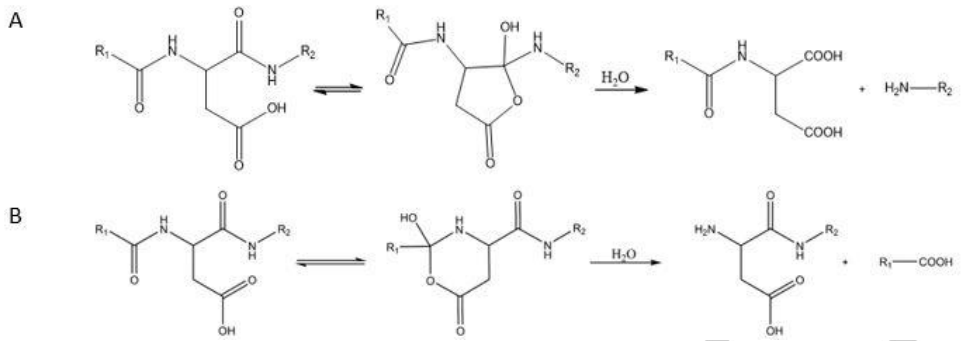

Figure 4 Reaction mechanism of the formation of the cyclic anhydride (top) and imide (bottom) intermediate and subsequent cleavage of the peptide bond. (Adapted from ref 4

pathway, the carboxylic group of the Asp side chain performs an intramolecular attack on the amide carbonyl carbon atom to form a cyclic hemiaminal intermediate that is labile in aqueous acidic media, resulting in a faster cleavage of X-Asp/Asp-X sites compared to linkages with other amino acids.[44] In our case, several control experiments, described below, unambiguously demonstrated that the combined Lewis and Brønsted acidity of the Hf_{18} catalyst are essential to the hydrolysis pattern observed, implying a dual role of Hf_{18} cluster in promoting the HHM hydrolysis. On one hand, its Lewis acidity activates the peptide bond favouring the formation of the hemiaminal intermediate 5, and on the other hand it can generate a local acidic environment that facilitates the disproportionation of this intermediate, resulting in an overall selective and efficient hydrolysis of the amide bond. In addition, detailed analysis of the supernatant by small angle X-ray scattering (SAXS), ESI-MS and ICP-OES, and UV-Vis spectroscopy investigation of the interactions between HHM and the Hf_{18} cluster further demonstrated that the superior reactivity of Hf_{18} for the HHM hydrolysis can be largely attributed to its heterogeneous nanocluster nature. Different control experiments have been performed in order to elucidate the role of **Hf_{18}** cluster in HHM hydrolysis. First of all, the high concentration of protons generated by **Hf_{18}** in solution does not afford the same hydrolysis pattern, evidencing the importance of **Hf_{18}** cluster Lewis acidity to the observed reaction. In our initial hydrolysis experiments, control samples providing identical conditions but lacking the **Hf_{18}** cluster indicated the importance of **Hf_{18}**, as no cleavage was observed after for 120 hours at 60 °C and pH 7.4 ( ). Moreover, upon increasing the buffer concentrations to avoid the pH decrease observed in reaction A-C), hydrolysis was also not observed. Therefore, additional control experiments were executed to investigate whether the observed HHM hydrolysis was due only to the high concentration of protons generated by the **Hf_{18}** cluster, or if the Lewis acidity was also necessary. To this end, an equivalent amount of **Hf_{18}** that was used in HHM hydrolysis experiments (2 µmol) was suspended in water and kept at 60 °C for 6 days. After **Hf_{18}** separation by centrifugation, the resulting supernatant, which had a pH of 2.52, was incubated with 0.02 mM HHM for 7 days. Even after 168 hours the SDS-PAGE analysis of the mixture showed presence of only three faint fragments, indicating slow and limited hydrolysis (See Figure S5), in sharp contrast with the outcome in the presence of **Hf_{18}**, which generated significantly more fragments in a shorter period. Together, these results indicate that the HHM hydrolysis illustrated in is not just the result of a mere Brønsted acid hydrolysis reaction, but likely derives from a synergistic actuation of the Lewis and Brønsted acidity provided by the **Hf_{18}** cluster.

The catalytically active species

The solid and insoluble nature of **Hf_{18}** cluster rather than smaller Hf-species is likely responsible for the hydrolysis pattern observed, as evidenced by further investigation of the supernatant prepared for the above control experiment. In addition to Brønsted acid-promoted hydrolysis of HHM, potentially soluble Hf species could play a role in the weak HHM hydrolysis that was observed upon its incubation with the supernatant in Figure S5. To investigate dissolution or leaching of **Hf_{18}** (i.e. as Hf_4), we analysed the **Hf_{18}** supernatant obtained after stirring **Hf_{18}** in water at 60°C for 6 days, by small angle X-ray scattering (SAXS), ESI-MS and ICP-OES. The SAXS experiments showed no significant scattering, suggesting that **Hf_{18}** clusters or other larger Hf-oligomers were not present in solution (Figure S6). Similarly, the ESI-MS experiments only showed the presence of some smaller (< 1000 m/z) species, which could be attributed to Hf dimers (Figure S7, Table S4). Furthermore, in ICP-OES measurements of the **Hf_{18}** supernatant detected only 3.03 ppm (± 2.4 %) Hf in solution, which corresponds to 0.05% of initial **Hf_{18}** cluster amount. Although these results indicate some Hf-dissolution under the reaction conditions (60°C, 6 days), the much slower hydrolysis observed in our control experiment, using this same supernatant, suggests solid **Hf_{18}** cluster is responsible for the hydrolytic activity observed in our initial experiments. Such conclusion is further supported by the robust interaction observed between the **Hf_{18}** cluster and HHM, discussed below.

Interaction between HHM and Hf_{18} cluster

HHM fast and persistent adsorption to the **Hf_{18}** cluster surface was confirmed by UV-Vis spectroscopy, and is consistent with the process of protein corona formation observed on the surface of nanoparticles. Such phenomena is attributed to mostly non-covalent van der Waals interactions, solvation forces, electrostatic and hydrogen bonding interactions.[46,47] The fading of HHM brown red colour observed in our initial hydrolysis experiments already suggested a strong interaction between the protein and the **Hf_{18}** cluster surface, prompting further investigation. HHM presence in solution can be conveniently tracked using UV-Vis spectroscopy, widely used to measure protein concentration in solution –the UV absorbance of tryptophan, tyrosine and phenylalanine amino acids at ca. 280 nm is an intrinsic property of proteins. Additionally, HHM possess a specific Soret band typically around 409 nm under physiological pH that originates from electronic $\pi \rightarrow \pi^*$ transition of its heme-group. Using water and HEPES buffer solutions, a rapid (< 10 min) and persistent disappearance of all HHM characteristic bands clearly indicate the protein had been completely removed from the solution (Figure S8).

The strong adsorption of HHM to the **Hf_{18}** cluster could be partially reversed by increasing the buffer concentration, indicating a stronger protein-cluster interaction happens at lower pH values. Addition of HEPES buffer partially inhibited adsorption of HHM to **Hf_{18}** surface so that in 50 mM HEPES ca 20 % of HHM was observed in solution after 1 hour, and this concentration remained stable over 24h. Increasing the HEPES buffer concentration to 100 mM and 200 mM resulted in 30 % and 57 % of HHM still being present in solution, respectively (Figure 5). To probe if this lower adsorption did not result from the intrinsic increase in ionic strength upon increasing the buffer concentration, 200 mM NaCl was added to an unbuffered suspension of 2 µmol **Hf_{18}** and 0.02 mM HHM at pH 7.0. However, HHM disappeared from solution after 30 minutes of incubation, suggesting ionic strength has a minimal effect on the adsorption process, and that the pH of the solution plays an important role. This major influence of pH on the adsorption process can be rationalized by the HHM loss of three-dimensional structure at low pH values ($2.3 < pH < 4.1$), likely increasing the number of sites able to interact with the **Hf_{18}** cluster. Previous NMR studies showed that HHM undergoes partial unfolding upon acidification of the medium. At pH = 4.1 the HHM adopts the molten globule state, in which much of secondary structure is retained, but the 3D fold is largely lost. Further lowering of pH results in a step-wise loss of both the tertiary and the secondary structure, yielding a flexible, partially unfolded structure,[48,49] thereby exposing more amino acid residues to the solution than in its original state.

Fate of Hf_{18} cluster after the reaction

In addition to the mechanistic study focusing on the protein and on the reactivity observed, we have also examined the **Hf_{18}** cluster for structural and reactivity changes after the hydrolysis reactions. Our attempt to recycle the **Hf_{18}** cluster after eluting the protein fragments from its surface with 1 % aqueous ammonia solution failed, as no cleavage was observed by SDS-PAGE upon incubation of recovered **Hf_{18}** with a new batch of HHM in water (60 °C, 24h, Figure S9). Further, this reaction mixture maintained its reddish colour, indicating that HHM also did not adsorb on the surface of the **Hf_{18}**. These results are in sharp contrast to the hydrolysis/adsorption of HHM observed with a freshly prepared **Hf_{18}**, and pointed to an overall 'deactivation of the cluster'. To understand if this 'deactivation' resulted from the reaction itself or the treatment with ammonia solution, we performed a thorough analysis of **Hf_{18}** before adding the ammonia solution. After the HHM hydrolysis reaction, the **Hf_{18}** cluster was separated from the reaction mixture by centrifugation and infrared (IR) spectroscopy, energy dispersive spectroscopy (EDS), and pair distribution function (PDF) of X-ray total scattering were used to evaluate any structural or compositional changes deriving only from the reaction conditions.

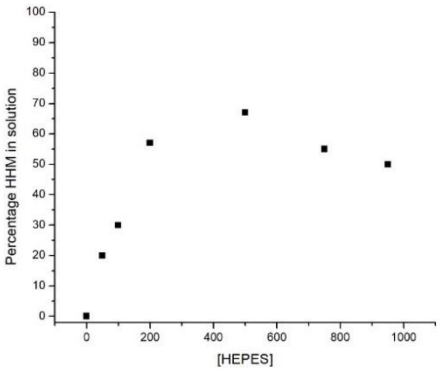

Figure 5 Percentage of HHM remaining in solution after incubation with **Hf_{18}** for 1 hour at 60°C at different HEPES concentrations. Percentage of HHM is based on the intrinsic aromatic absorbance at 280 nm.

Infrared (IR) analysis of the recovered **Hf_{18}** cluster after the HHM hydrolysis detected sulphate-phosphate exchange in phosphate

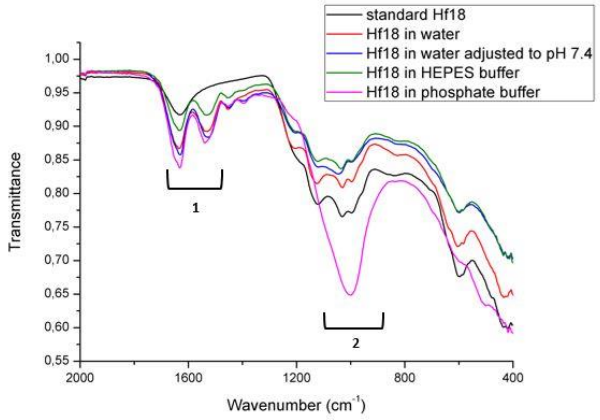

buffer condition, and confirmed HHM adsorption detected by UV-Vis spectroscopy analysis of the supernatant. In HEPES or water solutions, the sulfate bands remain consistently strong, but in presence of phosphate buffer a broad strong band appeared (950-1200 cm^{-1}), indicating an exchange of the labile sulphate ligands with phosphate in the **Hf_{18}** structure (Figure 6). This is in line with the low-coordinating capabilities of HEPES and strong coordinating character of phosphate buffer. Despite such ligand exchange, the hydrolysis of HHM was still observed (

B) in phosphate buffer, affirming **Hf_{18}** catalyst activity, regardless of the nature of the capping ligand. This is also consistent with the Hf-centres being the catalytic sites for the hydrolysis reactions. In addition, the IR spectra of recovered **Hf_{18}** revealed new bands in the region between 1450 and 1600 cm^{-1}, which are typical for amide stretches of proteins. This confirms HHM absorption to the **Hf_{18}** surface, consistent with the colour change of **Hf_{18}**, from white to red-brown upon reaction (See Figure S10). Finally, no observed sulfate-OH- exchange in HEPES buffered solutions is important for catalyst performance, since an abundance of hydroxyl ligands leads to condensation, aggregation, and loss of active surface sites.

Figure 6 IR spectrum of **Hf_{18}** sulphate cluster after 144 hours of reaction with HHM in different solution conditions. "Standard **Hf_{18}** cluster" is the as synthesized cluster, "**Hf_{18}** in water" was not adjusted prior to reaction, "**Hf_{18}** in water adjusted to pH 7.4" was adjusted to pH 7.4 prior to reaction. "**Hf_{18}** in HEPES buffer" and "**Hf_{18}** in phosphate buffer" are the **Hf_{18}** samples incubated in the corresponding buffer (20 mM, pH 7.4). **1** highlights the protein related amide stretches between 1450-1600 cm-1; **2** highlights the sulfate stretch of **Hf_{18}** and phosphate stretch (magenta spectrum).

While IR spectroscopy is informative of the fate of sulfate, phosphate and organic groups in the protein-**Hf_{18}** reaction, PDF provided information predominantly about the Hf-oxo core of **Hf_{18}**, since correlation peaks are dominated by the strongest scattering pairs, Hf-Hf, Hf-S and Hf-O. Figure 7shows the PDF of the **Hf_{18}** standard powder along with that which has been exposed to myoglobin (H_2O, 60°C, 6 days). The dominant peaks are the ~2.0-2.2 Å Hf-O bond and the ~3.5 Å Hf-Hf correlation of edge-sharing Hf-polyhedra. The remainder of the peaks represent numerous distances; likely where one atom is Hf, since scattering intensity scales with atomic number. Importantly, we note that 1) peaks are observed out to 11 Å, consistent with the longest Hf-Hf distance (and approximate diameter) of the cluster; and 2) there is little change in the **Hf_{18}**, before and after exposure to HHM in biological conditions. These studies confirm that the **Hf_{18}** is the heterogeneous catalysis responsible for hydrolysis of the HHM. With these same samples, we used EDS X-ray spectroscopy to semi-quantitatively determine Hf:S ratios in the pristine and post-exposed **Hf_{18}** samples. The pristine **Hf_{18}** has a ratio of 1.38, while the HMM-exposed **Hf_{18}** has a ratio of 1.34, indicating minimal change. The theoretical ratio from the crystal structure of **Hf_{18}** is 1.38.

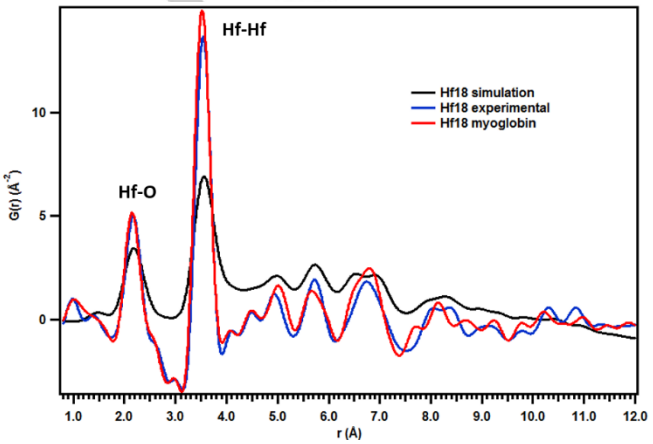

Figure 7 Pair distribution function (PDF) of **Hf_{18}** catalyst, pristine (blue) and after exposure to HMM, along with the simulated PDF for **Hf_{18}**. The minimal change between these two samples indicates the Hf-oxo core cluster remains intact upon exposure to the biological conditions.

Considering the above data confirms **Hf_{18}** stability in reaction conditions, it is logical to assume that the alkaline ammonia solutions used for the protein recovery caused inactivation of **Hf_{18}** catalysts, neutralising the acidity, and likely driving condensation reactions that inactivate undercoordinated Hf-centres. The pH of the **Hf_{18}** suspension recovered after addition of 1% ammonia had a pH around 9.5, in sharp contrast to the suspension of the fresh catalyst which had a pH around 3, strengthening this hypothesis. The IR spectrum of the recovered catalysts showed similarities to the phosphate incubated **Hf_{18}**, possibly indicating a change in the capping ligands which can result in the observed inactivity of recycled **Hf_{18}** (Figure S11). Exposure of used **Hf_{18}** to weak sulphuric acid to regenerate both the acidic terminal water ligands and the sulfate caps was not successful (Figure S12). Therefore, development of an alternative "elution protocol" in the future can probably circumvent the lack of recyclability, thereby largely expanding the applicability of **Hf_{18}** as a robust and effective heterogeneous artificial protease.

Conclusion

In this work, we demonstrate that a discrete hafnium (IV) polynuclear cluster, **Hf_{18}**, exhibits remarkable selectivity towards peptide bonds that contain Asp residues. Using HHM as a model protein substrate, a detailed mechanistic study showed that Lewis acidity of Hf^{4+} centres and Brønsted acidic surface of Hf_{18} were both essential for the hydrolysis to be observed, implying a dual role of the **Hf_{18}** in the peptide bond cleavage. Moreover, the fully heterogeneous nature of the reaction and the stability of the **Hf_{18}** cluster under the reaction conditions were also confirmed by thorough analysis of the supernatant and of **Hf_{18}** recovered from the reaction. To the best of our knowledge, this is the first report of selective protein hydrolysis using a heterogeneous discrete metal-oxo cluster, and highlights the great potential of insoluble metal-oxo cluster materials as inorganic proteases. Considering the enormous variety of available metal-oxo cluster based materials, we anticipate that our findings will open up new possibilities for their application as nanozymes that mimic proteases.

Acknowledgements

J.M. thanks the Academische Stichting Leuven. TPV thanks KU Leuven and Research Foundation Flanders (FWO) for funding. This research work was funded by the Ministry of Education, Science and Technological Development of the Republic of Serbia, GA No.OI172024, Serbian Academy of Sciences and Arts GA No. F-26 and the European Commission, under the Horizon 2020, FoodEnTwin project, GA No. 810752. Work performed at Oregon State University--synthesis of **Hf_{18}** and analysis of its solubility products (MA and KK)) and help in drafting the manuscript (MN) was supported by U.S. Department of Energy, Office of Basic Energy Sciences, Division of Material Sciences and Engineering, under award DE SC0010802.

Keywords: Heterogeneous Catalyst • Protein Hydrolysis • Amino acid Selective cleavage • metal-oxo cluster • artificial protease

References

[1] R. H. Rice, G. E. Means, W. D. Brown, *BBA - Protein Struct.* **1977**, *492*, 316–321.

[2] J. L. Proc, M. a Kuzyk, D. B. Hardie, J. Yang, D. S. Smith, A. M. Jackson, C. E. Parker, C. H. Borchers, *J Proteome Res* **2010**, *9*, 5422–5437.

[3] D. Li, W. Y. Teoh, J. J. Gooding, C. Selomulya, R. Amal, *Adv. Funct. Mater.* **2010**, *20*, 1767–1777.

[4] H. Sattar, A. Aman, U. Javed, S. A. Ul Qader, *Mol. Catal.* **2018**, *446*, 81–87.

[5] C. Bahamondes, G. Álvaro, L. Wilson, A. Illanes, *Process Biochem.* **2017**, *53*, 172–179.

[6] L. Tsiatsiani, A. J. Heck, *FEBS J* **2015**, *282*, 2612–2626.

[7] D. L. Crimmins, S. M. Mische, N. D. Denslow, *Curr Protoc Protein Sci* **2005**, *Chapter 11*, Unit 11.4.

[8] R. Kaiser, L. Metzka, *Anal. Biochem.* **1999**, *266*, 1–8.

[9] Y. Degani, A. Patchornik, *Biochemistry* **1974**, *13*, 1–11.

[10] H. N. Miras, J. Yan, D. L. Long, L. Cronin, *Chem. Soc. Rev.* **2012**, *41*, 7403–7430.

[11] S. S. Wang, G. Y. Yang, *Chem. Rev.* **2015**, *115*, 4893–4962.

[12] M. P. Santoni, G. S. Hanan, B. Hasenknopf, *Coord. Chem. Rev.* **2014**, *281*, 64–85.

[13] K. Stroobants, E. Moelants, H. G. Ly, P. Proost, K. Bartik, T. N. Parac-Vogt, *Chemistry (Easton).* **2013**, *19*, 2848–2858.

[14] K. Stroobants, G. Absillis, E. Moelants, P. Proost, T. N. Parac-Vogt, *Chem. - A Eur. J.* **2014**, *20*, 3894–3897.

[15] H. G. T. Ly, G. Absillis, R. Janssens, P. Proost, T. N. Parac-Vogt, *Angew. Chemie - Int. Ed.* **2015**, *54*, 7391–7394.

[16] A. Sap, L. Van Tichelen, A. Mortier, P. Proost, T. N. Parac-Vogt, *Eur. J. Inorg. Chem.* **2016**, 5098–5105.

[17] A. Sap, G. Absillis, T. N. Parac-Vogt, *Dalt. Trans.* **2015**, *44*, 1539–1548.

[18] G. Absillis, T. N. Parac-Vogt, *Inorg Chem* **2012**, *51*, 9902–9910.

[19] H. G. Ly, G. Absillis, T. N. Parac-Vogt, *Dalt. Trans* **2013**, *42*, 10929–10938.

[20] S. Vanhaecht, G. Absillis, T. N. Parac-Vogt, *Dalt. Trans* **2013**, *42*, 15437–15446.

[21] B. O. Keller, J. Sui, A. B. Young, R. M. Whittal, *Anal. Chim. Acta* **2008**, *7*, 71–81.

[22] J. Wu, X. Wang, Q. Wang, zhangping Lou, S. Li, Y. Zhu, L. Qin, H. Wei, *Chem Soc Rev* **2019**, *48*, 1004–1076.

[23] C. Hao, R. Gao, Y. Li, L. Xu, M. Sun, C. Xu, H. Kuang, *Angew. Chemie Int. Ed.* **2019**, 1–5.

[24] H. Wei, E. Wang, *Chem. Soc. Rev.* **2013**, *42*, 6060–6093.

[25] R. Bonomi, P. Scrimin, F. Mancin, *Org Biomol Chem* **2010**, *8*, 2622–2626.

[26] M. Diez-castellnou, F. Mancin, P. Scrimin, *J. Am. Chem. Soc.* **2014**, *136*, 1158–1161.

[27] L. Vandebroek, E. De Zitter, H. G. T. Ly, D. Conić, T. Mihaylov, A. Sap, P. Proost, K. Pierloot, L. Van Meervelt, T. N. Parac-Vogt, *Chem. - A Eur. J.* **2018**, *24*, 10099–10108.

[28] J. M. George, A. Antony, B. Mathew, *Microchim. Acta* **2018**, *185*, 1–26.

[29] D. Bobo, K. J. Robinson, J. Islam, K. J. Thurecht, S. R. Corrie, S. R. Corrie, *Pharm. Res.* **2016**, 2373–2387.

[30] V. A. Gritsenko, T. V Perevalov, D. R. Islamov, *Phys. Rep.* **2016**, *613*, 1–20.

[31] R. T. Frederick, J. M. Amador, S. Goberna-Ferrón, M. Nyman, D. A. Keszler, G. S. Herman, *J. Phys. Chem. C* **2018**, 16100–16112.

[32] J. Stowers, D. A. Keszler, *Microelectron. Eng.* **2009**, *86*, 730–733.

[33] J. T. Anderson, C. L. Munsee, C. M. Hung, T. M. Phung, G. S. Herman, D. C. Johnson, J. F. Wager, D. A. Keszler, *Adv. Funct. Mater.* **2007**, *17*, 2117–2124.

[34] S. Goberna-Ferrón, D. H. Park, J. M. Amador, D. A. Keszler, M. Nyman, *Angew. Chemie - Int. Ed.* **2016**, *55*, 6221–6224.

[35] J. A. Sommers, D. C. Hutchison, N. P. Martin, K. Kozma, D. A. Keszler, M. Nyman, *J. Am. Chem. Soc.* **2019**, *141*, 16894–16902.

[36] R. E. Ruther, B. M. Baker, J. H. Son, W. H. Casey, M. Nyman, *Inorg Chem* **2014**, *53*, 4234–4242.

[37] W. Mark, M. Hansson, *Acta Crystallogr.* **1975**, *31*, 1101–1108.

[38] J. H. Cavka, S. Jakobsen, U. Olsbye, N. Guillou, C. Lamberti, S. Bordiga, K. P. Lillerud, *J. Am. Chem. Soc.* **2008**, *130*, 13850–13851.

[39] S. Gopinath, P. S. M. Kumar, K. A. Y. Arafath, K. V. Thiruvengadaravi, S. Sivanesan, P. Baskaralingam, *Fuel* **2017**, *203*, 488–500.

[40] T. Suzukia, K. Imaib, *Cell. Mol. life Sci.* **1998**, *54*, 919–1004.

[41] J. B. Wittenberg, *J. Exp. Biol.* **2003**, *206*, 2011–2020.

[42] and J. A. V. A. H. A. V. D. O. J. J. W. A. P. Van Dam, *Eur. J. Biochem.* **1969**, *10*, 140–145.

[43] E. Derat, E. Lacote, B. Hasenknopf, S. Thorimbert, M. Malaeria, *J. Phys. Chem. A* **2008**, *112*, 13002–13005.

[44] C. Oliyai, R. T. Borchardt, *Pharm. Res.* **1993**, *10*, 95–102.

[45] A. Li, R. C. Sowder, L. E. Henderson, S. P. Moore, D. J. Garfinkel, R. J. Fisher, *Anal Chem* **2001**, *73*, 5395–5402.

[46] S. R. Saptarshi, A. Duschl, A. L. Lopata, *J. Nanobiotechnology* **2013**, *11*, 26.

[47] A. E. Nel, L. Mädler, D. Velegol, T. Xia, E. M. V Hoek, P. Somasundaran, F. Klaessig, V. Castranova, M. Thompson, *Nat. Mater.* **2009**, *8*, 543–557.

[48] J. T. Sage, P. M. Champion, D. Morikis, *Biochemistry* **1991**, *30*, 1227–1237.

[49] D. Eliezer, J. Yao, H. J. Dyson, P. E. Wright, *Nat. Struct. Biol.* **1998**, *5*, 148–155.

Entry for the Table of Contents

Layout 1:

RESEARCH ARTICLE

The discrete hafnium metal-oxo cluster ($Hf_{18}O_{10}(OH)_{26}(SO_4)_{13}(H_2O)_{33}$) (**$Hf_{18}$**) acts as a nanozyme for the strictly-selective hydrolysis of horse heart myoglobin (HHM) at Asp residues.

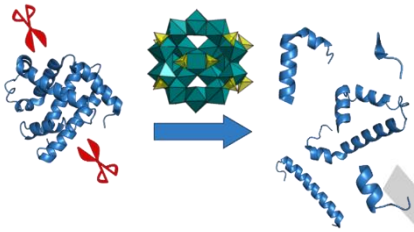

*Jens Moons, Francisco de Azambuja, Jelena Mihailovic, Karoly Kozma, Katarina Smiljanic, Mehran Amiri, Tanja Cirkovic-Velickovic, May Nyman, Tatjana N. Parac-Vogt**

Page No. – Page No.

Discrete Hf_{18} metal-oxo cluster as a heterogeneous nanozyme for site-specific protein fragmentation